Optics Letters

Intense stimulated Raman scattering in CO_2-filled hollow-core fibers

Katarzyna Krupa,[1,*] Kilian Baudin,[1] Alexandre Parriaux,[1] Gil Fanjoux,[2] and Guy Millot[1]

[1]Université Bourgogne Franche-Comté, ICB UMR CNRS 6303, 9 Avenue A. Savary, 21078 Dijon, France
[2]Université Bourgogne Franche-Comté, FEMTO-ST UMR CNRS 6174, 15B Avenue des Montboucons, 25030 Besançon, France
*Corresponding author: katarzyna.krupa@u-bourgogne.fr

Received 16 July 2019; revised 25 September 2019; accepted 3 October 2019; posted 3 October 2019 (Doc. ID 372813); published 29 October 2019

We demonstrate experimentally, the generation of an intense broadband comb-like spectrum spontaneously built up through stimulated Raman scattering in a low-pressure CO_2-filled hollow-core photonic crystal fiber pumped by a single infrared pump.

https://doi.org/10.1364/OL.44.005318

Frequency combs are of constant significant interest for their use in diverse areas of physics. Indeed, optical frequency combs have revolutionized precise optical frequency measurements by directly linking any optical frequency to a microwave clock. Today, they are also indispensable equipment for numerous other applications ranging from metrology to biomedical and environmental spectroscopy. One interesting technique to obtain multi-octave comb-like optical spectra is based on the generation of higher-order stimulated Raman scattering (SRS) in a hydrogen gas. Raman optical spectroscopy is one of the most common and widely used techniques offering multiple advantages, including non-destructive character, rapid measurement, no need for sample preparation, spatial resolution, and high chemical selectivity. Raman spectroscopy consists of focusing one or more intense laser beams in a gas under test in order to excite the rotational and/or vibrational modes of the gas molecules. The intensities of the excited spectral lines mostly depend on the power of the incident lasers, and the interaction length which, in free space, is limited to the Rayleigh length being in the order of a few millimeters only.

The development of hollow-core photonic crystal fibers (HC-PCFs) [1] has changed fundamentally the field of gas-based nonlinear optics allowing for observation many interesting new phenomena [2–4]. In gas-based SRS, low-loss HC-PCFs are capable of strongly reducing by several orders of magnitude the Raman threshold, in comparison to previous equivalent techniques using a gas cell, which have required a GW level of peak powers to generate SRS-based comb-like optical spectra [5,6]. Indeed, HC-PCFs make it possible to strongly confine together gases and a laser pump and guide them over several meters, hence, greatly increasing their interaction length. Thanks to these unique properties, since their development, HC-PCFs have attracted a lot of attention as an excellent candidate for the generation of highly efficient multi-octave Raman frequency combs. The generation of ultra-broad vibrational/rotational comb-like spectra through SRS has been widely studied, mostly in a hydrogen-filled HC-PCF [5,7–12]. The reported results show that, even though HC-PCFs have offered an unprecedentedly low threshold, the laser power required to generate intense Stokes and anti-Stokes Raman lines is still in the order of tens of kilowatts. The required pressure of a hydrogen gas can be reduced to the level of several bars by co-launching the pump pulse with a weak seed pulse at the Stokes frequency [13]. However, it remains relatively high in the order of tens of bars in the case of SRS starting from spontaneous Raman photons. Moreover, a serious inconvenience of using a hydrogen gas in a HC-PCF is a high hydrogen permeability of silica, which requires using special actions to protect the fiber from gas leakage. The interesting alternative allowing us to overcome these undesired and destructive issues is to use a CO_2 gas instead. Up to now, CO_2 has been used mostly to study the conditions to obtain efficient first-order anti-Stokes conversion in a relatively short 30 cm long HC-PCF, while it was chosen for its smaller Raman shift [14].

In this Letter, we study the ν_1 band of the $\nu_1/2\nu_2$ Fermi-dyad of CO_2 gas through SRS initiated from quantum noise in a HC-PCF, exploring its potential application for the generation of intense broadband comb-like spectra instead. The rovibrational Q-branch of the ν_1 band, shifted by 41.64 THz from the pump laser, is of fundamental interest because of its unique extremely narrow spectral width of the order of 300 MHz (at full width at half-maximum in intensity (FWHMI)) at around 1 bar of CO_2. Indeed, at the pressure of a few tens of millibars to 1 bar, this band undergoes a strong spectral compression due to combined effects of Dicke narrowing and collisional line-mixing. Moreover, although it is well-known that SRS of CO_2 is less efficient than that of hydrogen, interestingly, the Q-branch of CO_2 may exhibit a strong collapse, which makes this band very intense [15–17]. We will then demonstrate the generation of efficient Raman spectra through a spontaneous scheme by using a HC-PCF filled with CO_2 at a pressure not exceeding 6 bars and pumped by a single laser with a peak power not exceeding 40 kW.

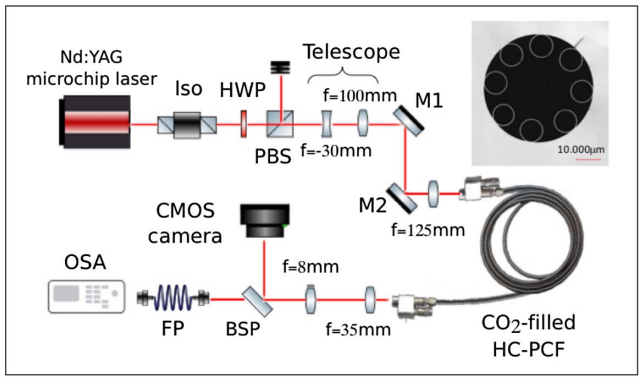

Fig. 1. Experimental setup to study SRS in a CO_2-filled HC-PCF. Iso, isolator; HWP, half-wave plate; PBS, polarization beam splitter; BS, non-polarizing beam splitter plate; M1 and M2, mirrors; FP, fiber patchcord; OSA, optical spectrum analyzer; HC-PCF, hollow-core photonic crystal fiber. Inset: SEM image of a HC-PCF delivered by GLOphotonics.

In our experiment, which is illustrated in Fig. 1, we used a photonic microcell system from GLOphotonics, namely, a 3 m long HC-PCF with a 30 µm of inner core diameter, terminated from both end sides by two gas-fillable cells filled with CO_2 gas with various pressure levels up to 6 bars. A cross-sectional image of the fiber recorded with an electron beam microscope is given in the inset of Fig. 1. As a pump beam, we chose a Nd:YAG microchip laser delivering ~450 ps pulses at 1064 nm, with a repetition rate of 1 kHz. We used a telescopic configuration to focus the linearly polarized Gaussian laser beam at the input face of the fiber with a FWHMI diameter of 23 µm. We also used a so-called *Z*-type scheme with two mirrors and a three-axis translation stage to adjust the position of the launched beam to be aligned with a fiber axis, while maximizing the coupling efficiency up to 39% (measured at 0.5 mbar of CO_2). We worked with a guided peak power not exceeding 40 kW. The output optical spectra were measured by using three optical spectrum analyzers (OSAs) covering the spectral range from 350 to 2400 nm. A complementary metal-oxide-semiconductor (CMOS) camera allowed us, instead, to verify the single-mode propagation conditions of our HC-PCF.

We started our investigation by measuring the ratio between input and output powers for various pressures of CO_2 in a HC-PCF. Figure 2 illustrates the total output peak power as a function of input peak power for a gas pressure ranging from 0.5 mbar up to 6 bars. We found that the input and output powers start to follow more and more parabolic behavior when the gas pressure grows larger. This deviation from a linear behavior, which is more pronounced for higher gas pressure, may be explained by additional losses caused by pressure-induced additional strains in the fiber. Note that the linear

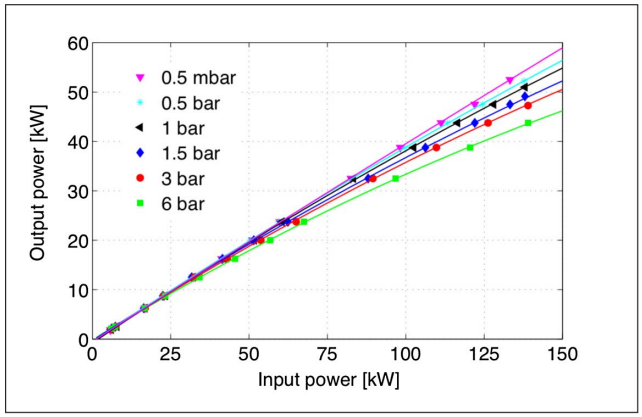

Fig. 2. Output power as a function of the input power measured for various pressures of CO_2 gas inside the HC-PCF.

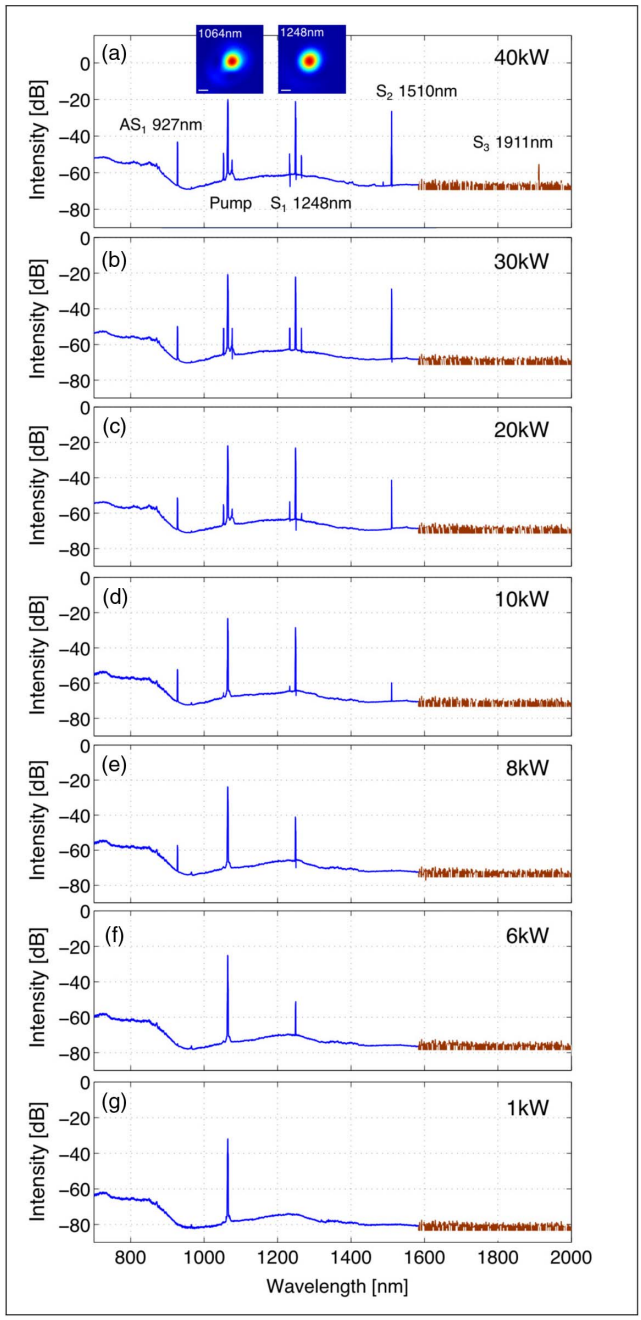

Fig. 3. Experimental spectra showing a Raman frequency comb generated at 6 bars of CO_2 gas pressure as a function of guided peak power ranging from 40 to 1 kW, as illustrated in panels (a)–(g), respectively. The blue and brown parts of the spectrum were measured with different OSAs. Insets: near-field patterns of the fiber output at the wavelengths of the pump laser and first Stokes beam. Scale bar: 10 µm.

losses of the HC-PCF structure are 0.09, 0.12, 0.21, 0.40, and 10 dB/m for the pump (1064 nm), the first anti-Stokes wave (927 nm), and the three consecutive Stokes waves (1248, 1510, and 1911 nm), respectively.

Next, we fixed the gas pressure at 6 bars, and we studied the evolution of the Raman spectra induced in a CO_2-filled HC-PCF. Panels (a)–(g) of Fig. 3 present the corresponding spectra as a function of guided pump peak power ranging from 40 down to 1 kW, respectively. As we can see, CO_2 gas allows for the generation of broadband comb-like spectra, which cover a spectral range of more than one-octave from 0.9 μm up to 2 μm. Remarkably, as illustrated in panel (a) of Fig. 3, only 6 bars of CO_2 pressure and 40 kW of peak power are enough to obtain three, spontaneously generated, Stokes sidebands (at 1248, 1510, and 1911 nm, respectively), with very intense first two lines and one anti-Stokes sideband (at 927 nm). Here the corresponding first and second Stokes sidebands were measured to be only 1.06 and 5.34 dB lower than the residual pump level, corresponding to 37% and 13.5% of conversion efficiency, respectively. We measured the corresponding powers with a power meter after proper spectral filtering. We also verified that the pump and induced Raman lines are carried by a fundamental mode of the fiber. The insets of panel (a) of Fig. 3 illustrate the corresponding near-field patterns of the fiber output measured at the wavelengths of a pump laser and first Stokes beam for the 40 kW peak power. Moreover, it is important to underline that at this relatively low CO_2 pressure, the quite intense first two Stokes lines can be obtained, even at pump power down to 10 [Fig. 3(d)] and 30 kW [Fig. 3(b)] for the first and second Stokes sidebands, respectively, i.e., at a lower power level than that required for H_2 gas at a few tens of bars. Note also that the Raman sidebands are very narrow, thus preserving the spectral finesse of the pump laser [15]. The additional low-intensity sidebands observed close to the pump and the first-order Raman Stokes wave may come instead from modulational instability induced by cross-phase modulation [18]. An analysis of an origin and dynamics of these spectral peaks is beyond the scope of this Letter, and it will be the subject of our next Letter. We also highlight that the impact of the input beam polarization state has been negligible.

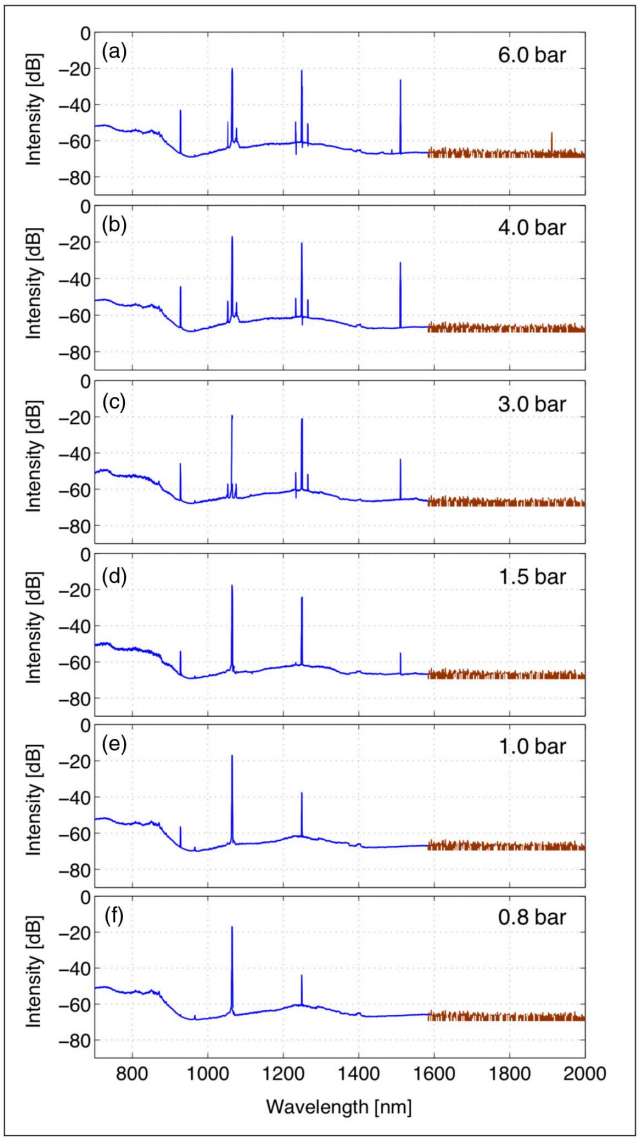

Fig. 4. Experimental spectra showing a Raman frequency comb generated at 40 kW of guided peak power as a function of CO_2 gas pressure ranging from 6 to 0.8 bars, as illustrated in panels (a)–(f), respectively. The blue and brown parts of the spectrum were measured with different OSAs.

Figure 4 presents the measurements of the Raman spectra generated in a CO_2-filled HC-PCF at 40 kW as a function of gas pressure. As we can see, at this moderate level of power, we can reduce the pressure of CO_2 gas down to 4 bars and still be able to generate first two Stokes sidebands with powers higher than the level of 10 dB below the pump power. Moreover, when increasing the guided pump power up to 47 kW, a first Stokes line can reach a power 10 dB lower than the pump level, even at CO_2 pressure as low as 1 bar. Here 47 kW is the maximum power available in our setup at this gas pressure.

Finally, in order to get additional insight and reproduce our experimental results, we performed split-step numerical simulations based on the 1 + 1D nonlinear Schrödinger equation, including chromatic dispersion, the Kerr effect, and the SRS effect, which reads as

$$\frac{\partial A}{\partial z}+\frac{i}{2}\beta_2\frac{\partial^2 A}{\partial t^2}+\frac{\alpha}{2}A=i\gamma(1-f_R)|A|^2A + i\gamma f_R A\int_0^\infty R(t)|A(z;\,t-t')|^2\mathrm{d}t', \tag{1}$$

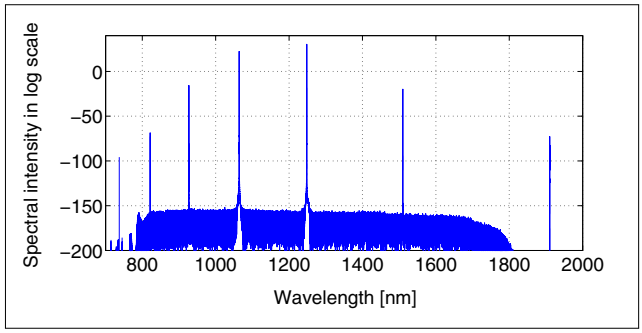

Fig. 5. Example of numerical spectrum generated at 29.12 kW of pump peak power.

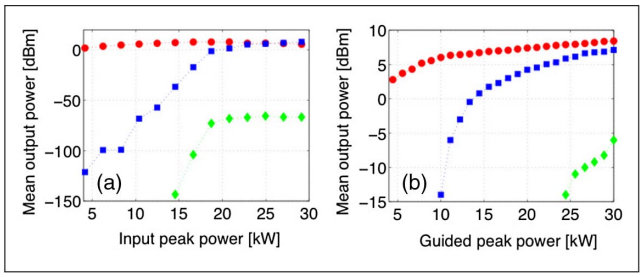

Fig. 6. Numerical [panel (a)] and experimental [panel (b)] power evolutions of various spectral components as a function of guided peak power. The red curve stands for the pump, the blue curve stands for the first-order Stokes, and the green curve stands for the second-order Stokes sidebands.

where $A(z;t)$ corresponds to the slowly varying envelope of the total electric field propagating in the z direction, β_2 is the group velocity dispersion (GVD) parameter from the dispersion curve given by the manufacturer, and α is the linear power attenuation of the fiber given by the manufacturer. $\gamma = 2\pi n_2/(\lambda A_{\text{eff}})$ corresponds to the nonlinear coefficient with $\lambda = 1064$ nm being the pump wavelength, $n_2 = 3.10^{-11}\,\mu\text{m}^2/\text{W}$ being the nonlinear index, and $A_{\text{eff}} = 416\,\mu\text{m}^2$ being the effective area of the fundamental mode of the optical fiber. We used a fiber length of 3 m and a pump pulse duration of 460 ps. The first term of the right-hand side of Eq. (1) corresponding to the Kerr effect leads to the self- and cross-phase modulation, together with the four-wave mixing processes. The second term accounts for the delayed Raman response represented in the time domain by the $R(t)$ function. Note that this Raman response is numerically modeled in the Fourier domain by one Raman gain band corresponding to a Lorentzian function with a bandwidth of 300 MHz and shifted from the pump by 41.64 THz. We considered the Raman gain in intensity equal to $1.1 \cdot 10^{-11}$ m/W. f_R is instead a parameter measuring the fractional contribution of Raman effects to the total nonlinearity, which according to our preliminary analysis does not significantly influence the spectral dynamics of SRS in CO_2-filled HC PCF. The detailed study of the corresponding impact of f_R will be the subject of our next Letter. An example of a numerical spectrum obtained at 29.12 kW is illustrated in Fig. 5, which accurately reproduces our measurements. Figure 6 instead presents the power evolution of various spectral components as a function of pump peak power, demonstrating again good qualitative agreement between the numerical [panel (a) of Fig. 6] and experimental [panel (b) of Fig. 6] results, in particular, concerning the pump and the first Raman Stokes wave. Observed discrepancies corresponding especially to the generation of experimentally much intense second Stokes sideband may be related to the value of Raman gain used in the simulations.

To conclude, we studied the nonlinear spectral dynamics of CO_2 gas spatially confined in a 3 m long HC-PCF. We focus on its ν_1 band of the $\nu_1/2\nu_2$ Fermi-dyad generated through spontaneously initiated SRS. We experimentally demonstrated that CO_2 gas can provide an interesting new low-pressure solution for the generation of efficient spectrally very narrow comb-like spectra, which is indeed non-permeable in silica. At only several bars of CO_2 pressure, we generated intense more than one-octave wide Raman spectra in the fiber pumped by a single laser at 1064 nm with a peak power not exceeding 40 kW. The exceptional fineness of the Raman band preserves the spectral width of the pump laser. Our numerical simulations accurately reproduced the experiments. Obtained results have a strong potential for application in numerous domains, including the development of novel high spectral finesse compact and powerful laser systems at new "*exotic*" wavelengths, which are not covered by existing gain media.

Funding. Agence Nationale de la Recherche (ANR-15-IDEX-0003, ANR-17EURE-0002); Institut Universitaire de France; iXcore research foundation.

Acknowledgment. The authors thank Jean Sauvage-Vincent from GLOphotonics and Alexandre Kudlinski for helpful scientific discussions.

REFERENCES

1. P. St.J. Russell, J. Lightwave Technol. **24**, 4729 (2006).
2. P. St.J. Russell, P. Holzer, W. Chang, A. Abdolvand, and J. C. Travers, Nat. Photonics. **8**, 278 (2014).
3. J. C. Travers, W. Chang, J. Nold, N. Y. Joly, and P. St.J. Russell, J. Opt. Soc. Am. B **28**, A11 (2011).
4. A. Nazarkin, A. Abdolvand, A. V. Chugreev, and P. St.J. Russell, Phys. Rev. Lett. **105**, 173902 (2010).
5. F. Couny, F. Benabid, P. J. Roberts, P. S. Light, and M. G. Raymer, Science **318**, 1118 (2007).
6. J. L. Domenech and M. Cueto, Opt. Lett. **38**, 4074 (2013).
7. F. Benabid, J. C. Knight, G. Antonopoulos, and P. St.J. Russell, Science **298**, 399 (2002).
8. Y. Y. Wang, C. Wu, F. Couny, M. G. Raymer, and F. Benabid, Phys. Rev. Lett. **105**, 123603 (2010).
9. F. Belli, A. Abdolvand, W. Chang, J. C. Travers, and P. St.J. Russell, Optica **2**, 292 (2015).
10. F. Benabid, G. Bouwmans, J. C. Knight, P. St.J. Russell, and F. Couny, Phys. Rev. Lett. **93**, 123903 (2004).
11. A. Abdolvand, A. Nazarkin, A. V. Chugreev, C. F. Kaminski, and P. St.J. Russell, Phys. Rev. Lett. **103**, 183902 (2009).
12. F. Tani, F. Belli, A. Abdolvand, J. C. Travers, and P. St.J. Russell, Opt. Lett. **40**, 1026 (2015).
13. A. Abdolvand, A. M. Walser, M. Ziemienczuk, T. Nguyen, and P. St.J. Russell, Opt. Lett. **37**, 4362 (2012).
14. Z. W. Barber, C. Renner, R. R. Reibel, S. S. Wagemann, Wm. R. Babbitt, and P. A. Roos, Opt. Express **18**, 7131 (2010).
15. B. Lavorel, G. Millot, R. Saint-Loup, H. Berger, L. Bonamy, J. Bonamy, and D. Robert, J. Chem. Phys. **93**, 2185 (1990).
16. B. Lavorel, G. Millot, R. Saint-Loup, H. Berger, L. Bonamy, J. Bonamy, and D. Robert, J. Chem. Phys. **93**, 2176 (1990).
17. C. Roche, G. Millot, R. Chaux, and R. Saint-Loup, J. Chem. Phys. **101**, 2863 (1994).
18. G. P. Agrawal, Phys. Rev. Lett. **59**, 880 (1987).